

TOPOGRAPHY OF CANDIDATE PHOENIX LANDING SITES FROM MOC IMAGES. R. L. Kirk¹, M. Rosiek¹, D. Galuszka¹, B. Redding¹, T. Hare¹, B. Archinal¹, and T. J. Parker², ¹U. S. Geological Survey, Flagstaff, AZ 86001, U.S.A. (rkirk@usgs.gov), ²Jet Propulsion Laboratory, Pasadena, CA 91109 USA.

Introduction: This abstract continues our series of reports [1-3] on high-resolution topographic mapping of martian terrains based on stereo and photoclinometric analysis of Mars Global Surveyor Mars Orbiter Camera narrow-angle (MGS MOC-NA) images [4]. Our initial efforts [1,2,5] were devoted to quantifying the topographic and slope hazards of candidate landing sites for the Mars Exploration Rovers (MER). Subsequent work has been funded by the NASA Critical Data Products (CDP) Initiative, and initially focused on providing high-resolution topographic data in support of the MARSIS and SHARAD sounding radar investigations [3]. Here, we report on further CDP-funded work to assess the topographic hazards of candidate landing sites for the 2007 Phoenix Lander.

Methodology: Our techniques for deriving topographic data by stereoanalysis and photoclinometry (PC) are described in detail elsewhere [5]. We use the USGS in-house digital cartographic software ISIS [6] for mission-specific data ingestion and calibration steps, as well as "2D" processing such as map-projection and image mosaicking, and photoclinometry [7]. Slope analysis is also performed with (unreleased) software that reads ISIS image files. Our commercial digital photogrammetric workstation running SOCET SET @ BAE Systems software [8] is used for "3D" processing steps such as control of the images and automatic extraction and manual editing of DEMs. SOCET SET includes a pushbroom scanner sensor model that is physically realistic but "generic" enough to describe most MOC-NA (and WA) images and allows low-order adjustments to register the images to the globally adjusted MOLA coordinates [9]. Many MOC images are also affected by high-frequency pointing variations ("jitter") that cannot be corrected with the available software for image control. Jitter in the stereobase direction gives rise to topographic artifacts in the form of stripes across the DEM; these can be suppressed by highpass filtering. Severe jitter at right angles to the stereobase interferes with matching; a workaround is to segment the image into regions that can be controlled and DEMs collected separately. MOC stereo DEMs may also contain artifacts in the form of a parabolic height variation across-track, caused by uncorrected optical distortions in the camera. Where present, such artifacts were modeled and removed with a polynomial fit.

The two-dimensional PC algorithm of Kirk [7] was used to construct DEMs of selected image regions with single-pixel resolution. Accuracy of these DEMs depends crucially on the validity of photometric assumptions, in particular, on the atmospheric haze contribution to a given image, which is essentially an unknown. Mis-estimating this haze level leads to errors in the overall scale of topography (and slopes). We therefore calibrate the PC analysis by choosing a haze estimate that gives results consistent with *a priori* topographic data (stereo or MOLA). Tests with simulated and real data suggest that photoclinometry calibrated in this way yields 10–20% relative accuracy for height differences and slopes [5].

Sites and Images: The Phoenix Lander is designed to touch down on the high northern latitudes of Mars, characterize the surface, acquire and analyze samples of soil and ice, and monitor atmospheric conditions [10]. Scientific and engineering criteria limit the candidate landing sites to the zone from 65°–72°N latitude. Within this zone, several 20°x7° regions were selected for intensive characterization and possible targeting, based primarily on initial estimates of subsurface ice abundance. Longitude ranges for the regions initially selected are A,

250°–270°E; B, 120°–140°E; C, 65°–85°E; and D, 230°–250°E. Region D was deselected following the first Phoenix Landing Site Workshop in December 2004. Regions A and C were eliminated following the third Workshop in November 2005 [11].

The geomorphologic diversity of the candidate landing sites for Phoenix is considerably less than that of the sites considered for MER [12]. Similar kilometer-scale features are seen in the lettered boxes, throughout the zone that contains them, and, indeed, over a somewhat wider range of latitudes. These include systems of ridges tens of km apart and hundreds of km in length (Panchaia Rupes); hills and knobs (including but not limited to Scandia Colles); km-scale polygons and other types of patterned ground; pedestal craters with ejecta and interiors elevated above the surrounding plains; and a small number of relatively fresh impact craters. These classes of features are resolved by MOLA altimetry [9], which indicates that the deepest craters measure no more than 300 m from floor to rim, and that the local relief of other features is 100 m. Superimposed on all these features is patterning at scales of a few tens of meters. Depending on the planform and the relative prominence of high regions versus the network of lows surrounding them, this decameter patterning may be described as "polygonal," "fingerprint," or "basketball" terrain in different areas. Albedo variations, mostly correlated with topography, are ubiquitous and have considerable impact on the photoclinometric analysis. Such variations include diffuse, low-albedo regions associated with hills, crater rims, and other high areas, and locally higher albedo in the troughs of the decameter patterned ground than on its protuberances.

The similarity of decameter and kilometer sized features over much of the northern lowlands is fortunate, because it reduces the number of distinct geomorphic and, in particular, hazard units [13] whose topographic properties must be characterized, and thus reduces the volume of image data required. Prior to the start of the Phoenix site selection process, the density of MOC images was lower at the latitudes of interest than elsewhere on Mars, and our database of validated stereopairs [3] contained only three pairs within the lettered regions. These are listed as Phoenix A1, C1, and D1 in Table 1. Useful pairs covering somewhat similar terrain were also found at the Viking 2 landing site (VL2) south of the Phoenix zone [3], and the site listed as Phoenix 0 to the north. This dearth of stereopairs is undoubtedly a direct result of the homogeneity of the northern plains. Fortunately, many of the images in this region, including most of those forming stereopairs, were targeted to impact craters. Local relief on these craters is generally the best available information for calibrating photoclinometry against the stereo results.

In support of the Phoenix site selection process, the MOC team targeted the lettered regions extensively during the period of relative atmospheric clarity from August 2004 through January 2005. Five additional stereopairs, designated Phoenix A2 and B1–B4, were obtained in this campaign and analyzed by us. Unfortunately, albedo variations in all these models (and also in C1 and D1) were so severe as to prevent us from obtaining useful results by PC. In general, decameter-scale albedo variations in the plains were noticeable but not severe; these would act to introduce spurious slopes into the photoclinometric DEMs but because the resulting slope distributions would systematically overestimate the true hazards, they might still have been useful for the hazard analysis. The

kilometer-scale diffuse dark areas associated with topographic highs posed a more serious problem, however, by preventing us from using the stereo-derived topography of these features to obtain atmospheric haze estimates and thus to calibrate the results of PC. Uncalibrated, our slope estimates could easily be in error by a factor of 2 or more, rendering them nearly useless.

The final set of results reported here were obtained by adopting a novel strategy to calibrate MOC images for photogrammetry. In the course of preparing base mosaics for hazard mapping [13], one of us (TJP) had examined all available MOC images in the candidate sites and registered all of those containing identifiable features to the MOLA DEM. This yielded a new and larger pool of candidate images not in stereopairs for which *a priori* topographic information was available. Of nine features in region B with promising MOLA relief for calibration and MOC image coverage, six were eliminated because of albedo variations or other problems. The remaining sites, Phoenix B5–B7, were analyzed to produce photogrammetric DEMs calibrated to MOLA. The B6 dataset is noteworthy because two overlapping images were available, with similar viewing angles (i.e., not providing useful stereo) but with illumination from opposite sides. We were able to register these images and form a ratio image from which albedo variations were largely eliminated. Such processing of visible-band images with differing illumination to eliminate albedo is a variant on the "magic airbrush" processing we have previously described for THEMIS VIS+IR data [14].

Results: Our stereo DEMs confirm the impression from MOLA that relief in the candidate landing sites is generally less than 100 m, but the effective resolution of at best 3 pixels (i.e., 10 or 20 m) is inadequate to resolve the decameter-scale patterned ground fully, leaving a concern that it might be dangerously rough over short distances. The photogrammetric DEMs do resolve decameter features, however, and demonstrate that the patterned ground does not roughen the surface dramatically over baselines between 3 and 10 m. RMS slopes over the shortest baseline measured for each site are summarized in Table 1. The range of values, 0.8°–4.5°, is comparable to results for the MER landing sites in Meridiani Planum (1.2°–2.5°) and Gusev cratered plains (2.3°–4.4°). Figure 1 shows the variation of slope with baseline in region B. The flatness of the curves for baselines <50 m indicates that there are no major slope hazards lurking at or just below the limit of resolution of our data. These results do not, however, constrain the hazards from features substantially smaller than our 3–10 m resolution, such as rocks. A combination of modeling and higher resolution images from the MRO HiRISE camera will be required to address this type of hazard.

Our results also provide information about slope distributions, in particular, the steepest slopes present. Requirements for safe entry, descent, and landing (EDL) by Phoenix include the absence of slopes in excess of 16° over any baseline (although the formal criterion for safety is the success of Monte Carlo simulations of landing on the topographic models we are supplying [15]). Slopes >16° are present over small areas near the rims of relatively fresh craters, but are not found on more subdued pedestal craters. In evaluating overall site safety, the entire mapped area of fresh craters (which constitute only a small fraction of the site) is likely to be considered "fatal", even though excessive slopes only occur on a small part of each crater.

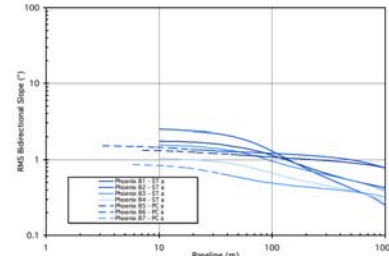


Figure 1. RMS bidirectional slope as a function of baseline for 7 MOC image sets in Phoenix candidate landing site region B.

Future Work: As this is written, the sun has returned to the latitudes of the Phoenix landing sites. Additional MOC images and stereopairs will be targeted in the three candidate landing site "boxes" within region B [11] as soon as the atmosphere clears sufficiently to allow useful imaging of the ground, in late spring 2006. HiRISE will also begin imaging the boxes with high priority once it begins operations in late fall 2006. Presuming the availability of support from an ongoing Critical Data Products Initiative, we expect to be involved in analyzing images from both sources to produce additional DEMs in support of the landing site selection and validation process.

References: [1] Kirk, R.L., et al. (2002) *LPS XXXIII*, 1988. [2] Kirk, R.L., et al. (2003) *LPS XXXIV*, 1966. [3] Kirk, R.L., et al. (2004) *LPS XXXV*, 2046. [4] Malin, M., and K.S. Edgett (2001) *JGR*, **107**, 23429. [5] Kirk, R.L., et al. (2003) *JGR*, **108**, 8088. [6] Eliason, E. (1997) *LPS XXVIII*, 331; Gaddis et al. (1997) *LPS XXVIII*, 387; Torson, J., and K. Becker, (1997) *LPS XXVIII*, 1443. [7] Kirk, R.L. (1987) Ph.D. Thesis, Caltech, Part III; Kirk, R.L., et al. (2003) *ISPRS-ET Workshop*, http://astrogeology.usgs.gov/Projects/ISPRS/Meetings/Houston2003/abstracts/Kirk_isprs_mar03.pdf. [8] Miller, S.B., and A.S. Walker (1993) *ACSM/ASPRS Annual Conv.*, **3**, 256; S.B., and A.S. Walker (1995) *Z. Phot. Fern.* **63**, 4. [9] Smith, D., et al. (2001) *JGR*, **107**, 23689. [10] Smith, P., et al. (2006) this conference. [11] Arvidson, R.E., et al. (2006) this conference. [12] Deal, K., et al. (2006) this conference. [12] Parker, T.J., et al. (2006) this conference. [14] Kirk, R.L., et al. (2005) *PE&RS*, **71**, 1167. [15] Guinn et al. (2006) this conference.

Table 1—MOC Image Sets Mapped for Candidate Phoenix Landing Sites and Analogs

Site	E Lon	Lat	Image 1	Image 2	Res 1 m	Emiss ang 1	Res 2 m	Emiss ang 2	RMS Slope	Baseline m	Description
VL2	134.1°	47.7°	M18-01458	E18-01397	1.81	0.11°	1.87	17.96°	4.14° 4.54°	6 1.8	ST SE of Viking landing site PC hilly subarea
PHX 0	196.8°	73.1°	E02-01891	R01-01314	3.02	0.36°	3.39	22.95°	0.45° 0.82°	115 3	MO km-scale polygons PC
PHX A1	251.9°	66.6°	M23-02019	E23-00945	7.31	0.19°	5.18	18.10°	2.99° 1.55°	21 5.2	ST outside crater ejecta PC
PHX A2	258.7°	68.7°	R22-01155	R23-00902	3.36	18.10°	4.33	31.31°	0.83°	12	ST subdued crater
PHX B1	130.4°	67.5°	R22-00168	S01-00644	3.35	18.16°	3.35	18.09°	1.78°	10	ST subdued crater
PHX B2	131.6°	67.4°	R22-00846	R23-00231	3.36	18.09°	4.23	30.02°	2.48°	10	ST hills
PHX B3	131.4°	67.0°	S01-00601	S02-00705	3.36	18.11°	6.36	30.20°	1.57°	10	ST hills
PHX B4	126.6°	66.8°	S01-00875	S02-00736	3.36	18.09°	4.56	33.62°	1.04°	10	ST hills
PHX B5	124.4°	67.6°	R20-01522		8.42	18.27°			1.33°	7.1	PC fresh crater ejecta
PHX B6	132.7°	67.8°	R23-00188	R21-00441	3.37	18.22°	3.36	18.13°	1.54°	3.1	PC pedestal crater, ratio image
PHX B7	132.7°	67.7°	R22-01248		3.37	18.14°			0.86°	5.8	PC ridge, subdued crater
PHX C1	64.9°	69.4°	M19-01733	E19-00409	5.99	0.38°	6.13	18.18°	1.46°	18	ST subdued crater ejecta
PHX D1	118.6°	68.1°	M00-00483	R19-02207	1.82	0.15°			4.40°	6	ST subdued crater

Res=Resolution in m/pixel across track. Emiss ang=emission angle. RMS Slope=Bidirectional root mean squared slope over given baseline. Description includes type of topographic data: MO=MOLA altimetry, ST=stereo, PC=photogrammetry.